

HYPERSONIC TURBULENT NON-EQUILIBRIUM REACTIVE NOZZLE FLOW CALCULATIONS

F. Leclère

SNECMA Villaroche, RD 57 Réau, 77556 Moissy-Cramayel Cedex, France
ONERA-CERT-DERAT, 2, avenue E. Belin B.P. 4025, 31055 Toulouse Cedex, France

B. Aupoix

ONERA-CERT-DERAT, 2, avenue E. Belin B.P. 4025, 31055 Toulouse Cedex, France

Abstract

Boundary layer flows at the combustion chamber exit of an hypersonic air-breathing plane are studied for two cruise speeds of Mach 6 and 12. Along the nozzle, the flow is reactive and the chemical mechanism can comprise over one hundred reactions and fifteen species. The number of chemical reactions is reduced by considering, as a single reaction, reactions which differ only from their catalyst and whose reaction rates are proportional. Moreover, reactions with very little influence on the production term are neglected. Chemistry-turbulence coupling is approached with two completely different ways. If the flow at the scramjet exit is well mixed, temperature fluctuations have a strong influence on reaction rates which are exponential functions of temperature. This dependency is taken into account by using a second order series expansion in $\sqrt{t't'}/\bar{T}$ or by using assumed Gaussian PDF. Both methods are completely different but their actions are identical. Conversely, if the flow is unmixed, chemistry is limited by the turbulent mixing time necessary for species to be in contact and an Eddy-Break-Up model permits to express the production terms. This approach seems to over limit chemical kinetic and the flow reaches a frozen state.

Introduction

Hypersonic air-breathing propulsion systems require a long nozzle that must be integrated within the airframe. Turbulent chemical processes persist throughout the nozzle and attention will be focused here on two-dimensional boundary layer flows. Finite rate

chemistry has to be considered, consequently non-equilibrium turbulent reacting flows must be investigated.

Turbulent boundary layer computations

Governing equations

At very high temperature, the gas is subjected to chemical reactions and the mixture composition evolves. In order to use different fuel mixtures, a boundary layer code has been developed which allows the use of arbitrary chemical species.

The fluid is compressible and fluctuations exist for pressure and velocity but also for temperature, density, mass fractions... A stationary flow is studied and Favre average permits to express boundary layer equations in a form similar to the incompressible one. Any instantaneous quantity, q is divided into a mean value, \bar{q} and fluctuations, q' . Turbulence closure relations are required to model the fluctuations correlation.

Continuity and momentum equations are written as usual. Each of the N species composing the multicomponent mixture verifies the species conservation equation. Stagnation enthalpy at the outer edge of the boundary layer is constant and it is therefore very convenient to write energy equation for this variable. Transport coefficients and thermodynamic properties require the knowledge of the temperature throughout the whole computational field. But, for high temperature gas, the relation between enthalpy and temperature is not simple. Thus it is sometimes more adequate to write the energy equation for the temperature to represent chemically non-equilibrium but thermally equilibrium flows.

Thermodynamic properties

Thermodynamic species properties, such as specific heat, enthalpy and standard entropy are fitted by polynomial functions of temperature from Chemkin's data base⁽¹⁰⁾ for a temperature range from 300 K to 7000 K.

Every species is considered as a perfect gas and verifies the state equation of perfect gases and mixture pressure is calculated according to the Dalton law.

Transport properties

Interaction force between molecules derives from a potential and the most usual one is the Lennard-Jones potential. Collision integrals $\Omega_{IK}^{(1,1)*}$ and $\Omega_{IK}^{(2,2)*}$ permit to determine transport coefficients and are modelled by Hattikudur and Thodos⁽⁸⁾.

Diffusion coefficients for a multicomponent gas mixture are expressed according to the exact kinetic theory proposed by Hirschfelder, Curtiss and Bird⁽⁹⁾. In the studied boundary layer flows, temperature is under 4000 K and the formulations of Wilke⁽¹⁷⁾ for the viscosity and of Mason and Saxena⁽¹¹⁾ for the thermal conductivity are accurate enough. Internal degrees of freedom of molecules create internal mixture conductivity which is given by the Eucken correction. Thermal diffusion effects, which are second order effects, are neglected.

Turbulence modelling

The turbulence models used are that of Chien⁽³⁾ and that of Nagano and Tagawa⁽¹²⁾ which are two-equation ($k - \varepsilon$) models. Both used the concept of eddy viscosity :

$$\mu_t = C_\mu f_\mu \frac{k^2}{\varepsilon}$$

where $C_\mu = 0.09$ and f_μ is the damping function, which depends upon the chosen model of turbulence.

Chemistry-turbulence interaction required the knowledge of the temperature variance. This variance and its dissipation rate ε_t , are solved using a two-equation model for heat transfer developed by Youssef, Nagano and Kim⁽¹⁸⁾. But this formulation is not well adapted to high Mach number and strong pressure gradients flows. Thus, to avoid this problem, a simpler relation given by Gaviglio⁽⁷⁾, is used to express $\overline{t't'}$ in term of kinetic energy

and velocity and temperature gradients.

$$\sqrt{\overline{t't'}} \frac{\partial u}{\partial y} = \sqrt{k} \frac{\partial T}{\partial y}$$

Boundary conditions

Initial profiles are determined by a self similar solution whose outer edge conditions are those found at the scramjet exit. Inviscid flow solutions at the wall impose the outer edge conditions of the boundary layer.

All computations have been made with an imposed wall temperature of 1000 K. Wall species mass fractions depend on the wall material which tends to catalyse, more or less, chemical reaction. If the wall is fully catalytic, reaction rates are infinite and the mixture composition correspond to the chemical equilibrium for a temperature of 1000 K and the given pressure. On the contrary, for a non-catalytic wall, mass diffusion fluxes of species are equal to zero and then species mass fraction gradients, at the wall, are null.

Chemical mechanisms

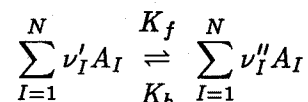
Complete mechanisms

Hydrogen burning scramjets are considered here. Reaction mechanisms of hydrogen-air chemistry were chosen in order to cover the range of gas compositions and the temperature and pressure variations expected during the nozzle expansion process.

In a very detailed form, the reaction mechanism consists of a set of eighty-five reactions and fifteen species proposed by Sangiovanni, Barber and Syed⁽¹⁴⁾. The different species are those present in the air (N_2 , O_2 , N , O , NO , N_2O , NO_2 and Ar), the hydrogen (H_2) and the products of its combustion (H , OH , H_2O , HO_2 , H_2O_2 and HNO). Another model, compound of one hundred and nine reactions and the same species, has been proposed by Evans and Schexnayder⁽⁵⁾.

Chemical non-equilibrium

In its most general form, a chemical reaction involving N different species is expressed, according to Penner's notations :



ν_I' and ν_I'' are the stoichiometric coefficients of forward and backward reactions and the chemical symbol of species I is A_I .

For a mechanism of R reactions, total production term of species I is equal to the sum of every reaction production term.

$$\dot{\omega}_I = \sum_{r=1}^R M_I (\nu_{I_r}'' - \nu_{I_r}') * \left(K_{f_r} \prod_J n_J^{\nu_{J_r}''} - K_{b_r} \prod_J n_J^{\nu_{J_r}'} \right)$$

where n_J is the species concentration.

Reaction rates are given according to the non-Arrhenius law :

$$K = AT^\alpha \exp\left(-\frac{E_A}{RT}\right)$$

where E_A is the activation energy. Constants A and α are obtained experimentally and, as their determination is very difficult, differences of several orders of magnitude are observed in the literature.

For a given thermodynamic state, a multi-component gas mixture tends towards chemical equilibrium. Then production terms are equal to zero and forward and backward reaction rates are no longer independent. So, if constants, indispensable to calculate backward reaction rate are not available, this rate is determined by :

$$K_{eq} = \frac{K_f}{K_b}$$

The equilibrium constant depends on the thermodynamic properties of the gas.

$$K_{eq} = \left(\frac{p_{ref}}{RT}\right)^{\sum_{I=1}^N (\nu_I'' - \nu_I')} \exp\left(\frac{A}{RT}\right)$$

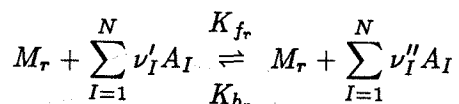
where p_{ref} is the reference pressure of 101325 Pa. The affinity of the reaction, for the reference pressure :

$$A = - \sum_{I=1}^N (\nu_I'' - \nu_I') G_I$$

is a function of the standard Gibbs free enthalpy.

Reaction with several catalysts

Considering a set of R reactions which differ only from their catalyst M_r :



and whose reaction rates are proportional to the reaction rates of the chemical reaction with no catalyst (indexed with "0" sign).

$$K_{f_r} = E_r K_{f_0}, \quad K_{b_r} = E_r K_{b_0}$$

where E_r is the efficiency of the catalyst M_r . The higher E_r is the more M_r catalyses the reaction.

Then the production term of the set of R reactions is also proportional to the production term of the reaction with no catalyst.

$$\dot{\omega}_I = \sum_{r=1}^R \dot{\omega}_{I,r} = \dot{\omega}_{I,0} \underbrace{\sum_{r=1}^R E_r n_{M_r}}_E$$

This way of writing production terms allows to reduce computation time by considering the set of R reactions as a single reaction with a corrective term E for the determination of the production term. This method decreases the two previous reaction mechanisms to respectively forty nine and twenty five reactions, but the number of different species remains the same.

Reduced chemical model

In order to reduce, once more, the number of chemical reactions, reactions whose production terms are very small in comparison with other reactions production terms are neglected.

Let $\dot{\omega}_{I,r}(x, y)$ be the production term of species I in the reaction r at an abscissa x and an ordinate y . Considering the maximum of production term of species I in all chemical reactions, at the point of co-ordinates x, y :

$$Max_1(I, x, y) = \max_{r=1, R} [\dot{\omega}_{I,r}(x, y)]$$

and the maximum of $Max_1(I, x, y)$ for the whole profile at the given abscissa x :

$$Max_2(I, x) = \max_{0 < y \leq \delta} [Max_1(I, x, y)]$$

$\dot{\omega}_{I,r}(x, y)$ is not negligible if it simultaneously satisfies the two following inequalities :

$$\left| \frac{\dot{\omega}_{I,r}(x, y)}{Max_1(I, x, y)} \right| > S_1$$

$$\left| \frac{\dot{\omega}_{I,r}(x, y)}{Max_2(I, x)} \right| > S_2$$

where S_1 and S_2 are adjustable constants. Values of 10% for S_1 and 1% for S_2 constitute a good compromise between computation time and accuracy. Reaction r is suppressed if its production terms are always negligible for any species, and throughout the whole computation field.

Turbulence-Chemistry coupling

An important physical effect in turbulent reacting flows is the interaction between turbulence and chemistry. As fast combustion is not involved, quite simple models of turbulence-chemistry coupling are considered.

Series expansion

If the fluid is assumed to be well-mixed, the chemical reaction rate, which depends on the usual non-Arrhenius type function, can be written in terms of the mean and fluctuating components of temperature and rewritten using a second order series expansion of Taylor.

The modified reaction rate term becomes, according to Borghi⁽²⁾ or to Narayan and Girimaji⁽¹³⁾:

$$\begin{aligned} \widetilde{K}(T) &= \left(1 + m \frac{\widetilde{t'^2}}{\widetilde{T}^2}\right) A \widetilde{T}^\alpha \exp\left(-\frac{E_A}{\widetilde{RT}}\right) \\ m &= (\alpha - 1) \left(\frac{\alpha}{2} + \frac{E_A}{\widetilde{RT}}\right) + \frac{1}{2} \left(\frac{E_A}{\widetilde{RT}}\right)^2 \end{aligned}$$

Most of the time, reaction of combustion of H_2 have a positive m and the H_2 combustion rate is therefore increased by the turbulence.

If backward reaction rate is not expressed by a non-Arrhenius law, it is equal to the ratio of forward reaction rate to the equilibrium constant. The backward reaction rate is then written:

$$K_b(T) = A_b T^{\alpha_b} \exp\left(-\frac{E_{A_b}}{RT}\right)$$

where:

$$\begin{aligned} A_b &= A_f \left(\frac{p_{ref}}{\mathcal{R}}\right)^{-\sum_{I=1}^N (\nu_I'' - \nu_I')} \\ \alpha_b &= \alpha_f + \sum_{I=1}^N (\nu_I'' - \nu_I') \\ E_{A_b} &= E_{A_f} - \sum_{I=1}^N (\nu_I'' - \nu_I') G_I \end{aligned}$$

It must be pointed out that this is not a real non-Arrhenius law because the energy E_{A_b} is no longer a constant but is a function of temperature.

Using the Van't Hoff relation:

$$\frac{\partial \left(\frac{G_I}{T}\right)}{\partial T} = -\frac{H_I}{T^2}$$

a second order series expansion of Taylor of the backward reaction rate is obtained. It has the same form as the expression proposed by Narayan but with a different factor m_b .

$$\begin{aligned} m_b &= (\alpha_b - 1) \left(\frac{\alpha_b}{2} + \frac{E_{A_b} + \beta}{\widetilde{RT}}\right) \\ &+ \frac{1}{2} \left(\frac{E_{A_b} + \beta}{\widetilde{RT}}\right)^2 + \gamma \end{aligned}$$

where:

$$\begin{aligned} \beta &= \sum_{I=1}^N (\nu_I'' - \nu_I') (G_I - H_I) \\ \gamma &= -\frac{1}{2\mathcal{R}} \sum_{I=1}^N (\nu_I'' - \nu_I') C_{pI} \end{aligned}$$

Additional coefficients β and γ are functions of temperature and may strongly modify the value of m_b . If they are neglected, backward reaction rate can even vary of several orders of magnitude.

Probability density function

Another way of taking into account temperature fluctuations is to use probability density function (PDF). As temperature is never negative, mean reactions rate are determined as follows:

$$\widetilde{K}(T) = \int_0^\infty K(T) P(T) dT$$

Gaussian PDF is appropriate for incompressible flows and, as little information is available on compressible flows, an assumed Gaussian PDF was chosen.

$$P(T) = \frac{1}{\sqrt{2\pi\widetilde{t'^2}}} \exp\left[-\frac{(T - \widetilde{T})^2}{2\widetilde{t'^2}}\right]$$

The Gauss-Hermite formula⁽¹⁵⁾ provides a powerful approximate method to determine

such an integral as :

$$\begin{aligned} \tilde{f}(x) &= \int_{-\infty}^{\infty} f(x) \exp(-x^2) dx \\ &\simeq \sum_{i=1}^n A_i (f(x_i) + f(-x_i)) \end{aligned}$$

Applied to the reaction rate it becomes :

$$\bar{K}(T) \simeq \frac{1}{\sqrt{\pi}} \sum_{i=1}^n A_i [K(T_i^+) + K(T_i^-)]$$

where :

$$\begin{cases} T_i^+ = \bar{T} + \sqrt{2t't'}x_i \\ T_i^- = \bar{T} - \sqrt{2t't'}x_i \end{cases}$$

x_i are given in rising order and the lower temperature is then :

$$T_{min} = \bar{T} - \sqrt{2t't'}x_n$$

As the degree n of the polynomial increases, x_n increases too. Since a negative temperature has no physical meaning, x_n cannot exceed a maximum authorised value and the degree of the polynomial is thus limited.

Forward reaction rate of reaction of dissociation of hydrogen, for different degrees of the Gauss-Hermite polynomial, is shown on figure 1.

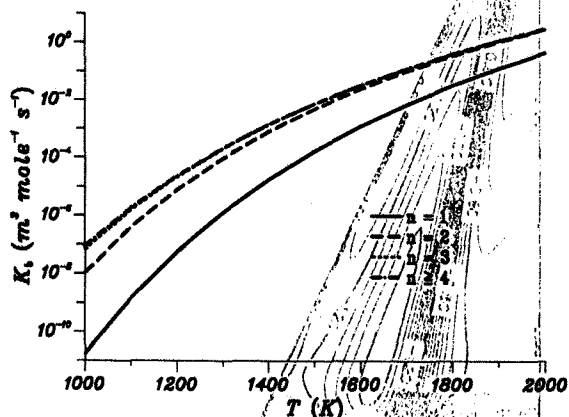


Figure 1: Forward reaction rate of reaction : $H_2 + M \rightleftharpoons 2H + M$ for polynomial of degree n

It can be seen that a polynomial of degree under three is not accurate enough. For higher degrees, curves are merged. A polynomial of degree five is generally chosen as a good compromise between accuracy and computation time.

Comparison between the two approaches

Mean reaction rates of the reaction :



are given on figures 2 and 3. Reaction rates obtained with temperature fluctuations are compared to the reaction rate at the mean temperature.

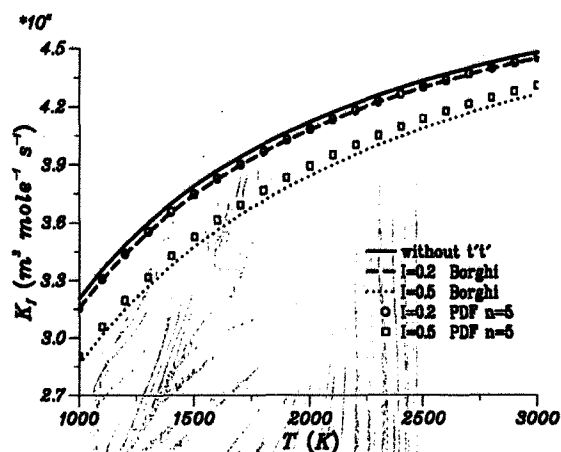


Figure 2: Forward reaction rate of reaction : $2 OH \rightleftharpoons O + H_2O$

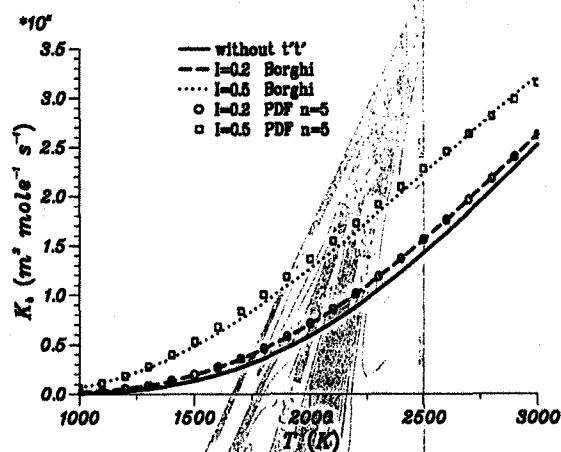


Figure 3: Backward reaction rate of reaction : $2 OH \rightleftharpoons O + H_2O$

Two fluctuation intensities, $I = \sqrt{t't'}/\bar{T}$, of 20% and 50% are studied. Assumed Gaussian PDF and Taylor second order series expansion (labelled Borghi) are in good agreement and a slight difference is seen only for an intensity level of 50% which is too important to have real physical meaning.

If the reaction rate curve is convex then the mean reaction rate is lower than the rate obtained for the mean temperature. This effect

is shown on figure 2. On the contrary, for a concave curve such as on figure 3, opposite effect can be observed.

Second order series expansion of backward reaction rate was computed using the equilibrium constant and the extension of the formulation proposed by Narayan. It can be noticed that if the backward reaction rate is expressed by :

$$\begin{aligned}\widetilde{K}_b(T) &= \frac{\widetilde{K}_f(T)}{K_{eq}(\widetilde{T})} \\ &= \left(1 + m_f \frac{\widetilde{t}'_f}{\widetilde{T}^2}\right) K_b(\widetilde{T})\end{aligned}$$

then the curvature of the forward reaction rate imposes the way temperature fluctuations affect the mean backward reaction rate. Concerning the previous chemical reaction, it leads to a decreasing of the mean backward reaction rate whereas the opposite effect is expected.

Eddy-Break-Up

If the fluid is assumed to be unmixed, the turbulence-chemistry interaction can be described by the Eddy-Break-Up model proposed by Spalding ⁽¹⁶⁾. Indeed, when the chemical reaction rate depends on the non-Arrhenius law which is a function of the temperature, the value of the reaction rate is overestimated. A better agreement is obtained when the local reaction rate is limited by the rate of break-up of lumps of unburned gas.

Considering a one-step irreversible reaction of combustion of fuel F in oxidant O which gives product P :



The production term of the fuel is expressed by :

$$\dot{\omega}_F = \alpha C_{ebu} \rho \frac{\varepsilon}{k} \sqrt{c'c'}$$

The variance of mass fraction $\widetilde{c'c'}$ can be defined as follows :

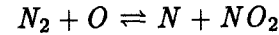
$$\widetilde{c'c'} = \beta \tau (1 - \tau)$$

where τ is the reactedness of the reaction. $\tau = 0$ for unburnt mixture and $\tau = 1$ for fully burnt mixture.

$$\tau = \frac{C_F - C_{F,i}}{C_{F,f} - C_{F,i}}$$

where i stands for initial state and f for final state.

For a much more complex reaction mechanism, a close study of each reaction must be done in order to decide if this reaction is subjected to an EBU model. For example, the following reaction :



does not involved a fuel and an oxidant and thus is not affected by EBU.

If EBU model is applied, as the code cannot know which species is an oxidant or a fuel or a product of combustion, a more general expression of the variance of mass fraction is proposed :

$$\widetilde{c'c'} = \beta \frac{\min_{\nu'_I \neq 0} [C_I (1 - C_I)]}{S (1 - S)}$$

where S is the sum of mass fraction of species involved in the right hand side of the reaction.

$$S = \sum_{\nu'_I \neq 0} C_I$$

and $\alpha \beta C_{ebu}$ is an adjustable constant with a standard value of 4.

Results

Test cases

Several hypersonic flight conditions with cruise speeds between Mach 6 and 12 are proposed in table 1. Two cases corresponding to cruise speeds of Mach 6 and 12 were chosen for this scramjet nozzle study. Geometry of the two-dimensional nozzle is shown on figure 4.

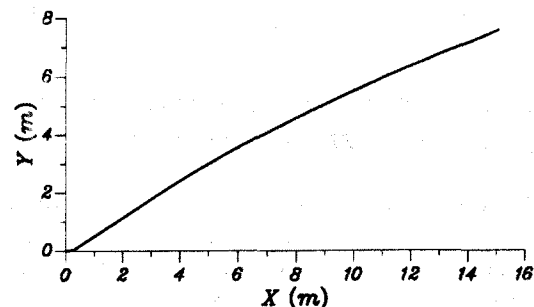


Figure 4: Nozzle geometry

<i>Mach</i>	6	8	10	12
T (K)	2621	2576	2148	2000
P (bar)	1.35	0.74	0.51	0.4
T_t (K)	2918	3237	3359	3627
P_t (bar)	3.4	6.2	11.2	22.8
richness	1	1	2	2.5
$\eta_{comb.}$	0.9	0.87	0.83	0.8
ρ ($kg\ m^{-3}$)	0.15	0.082	0.053	0.04
γ	1.161	1.159	1.245	1.264
C_p (J/kg/K)	3390	3483	2392	2460
V ($m\ s^{-1}$)	1350	2097	2811	3448
<i>Mach</i>	1.31	2.05	2.56	3.06
\dot{m} ($kg\ s^{-1}$)	125	107.5	95.7	90.2

Table 1: Aerothermodynamic specifications at the scramjet exit

	$M = 6$	$M = 12$
H_2	0.50	4.56
O_2	3.40	4.32
H	0.02	0.01
O	0.14	0.00
H_2O	19.91	19.42
N_2	73.10	70.42
OH	0.99	0.01
NO	0.63	0.00
Ar	1.30	1.25

Table 2: Chemical composition (%)

Temperature, pressure and velocity at the scramjet exit are given in table 1 and gas mixture in species mass fractions, at the scramjet exit, are given in table 2.

Mach distributions along the nozzle wall were taken from the results of previous inviscid flow computations done by the French engine constructor SNECMA and are shown on figure 5.

Reduced chemical model

The set of two inequalities proposed to neglect chemical reactions has been tested on the STS2 shuttle hypersonic re-entry⁽⁴⁾. The air dissociation in the boundary layer is described

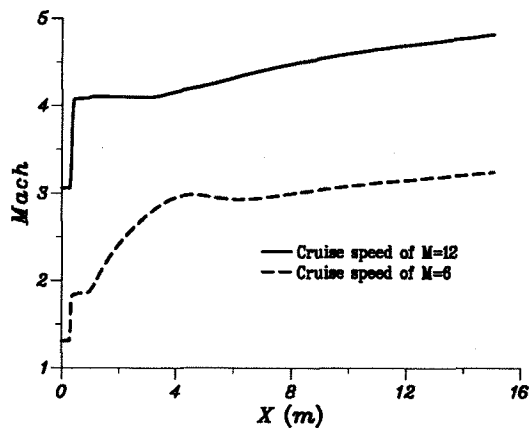


Figure 5: Mach distribution along the wall

by the well known chemical mechanism of seventeen reactions and five species (N_2 , O_2 , NO , N and O) provided by Gardiner⁽⁶⁾. When applied, the previous method yields a set of three reactions which corresponds to the simplified model proposed by Zeldovich.

Those criteria, applied to the chemical models of hydrogen-air combustion, proposed by Sangiovanni⁽¹⁴⁾ and by Evans⁽⁵⁾, lead to one and the same mechanism of eight reactions and ten species (N_2 , O_2 , N , O , NO , Ar , H_2 , H , OH and H_2O) given on table 3.

$O_2 + H \rightleftharpoons OH + O$
$H_2 + O \rightleftharpoons OH + H$
$2 OH \rightleftharpoons H_2O + O$
$H_2 + OH \rightleftharpoons H + H_2O$
$H_2 + M \rightleftharpoons 2 H + M$
$OH + H + M \rightleftharpoons H_2O + M$
$N_2 + O \rightleftharpoons N + NO$
$H + NO \rightleftharpoons N + OH$

Table 3: Reduced chemical model

Figures 6 to 8 compare production terms for different species and abscissas, between Sangiovanni model, Evans model and the simplified version of Sangiovanni model. Forward reaction rates of the simplified model are determined by the non-Arrhenius law constants provided by Sangiovanni. They may greatly differ from the reactions rates proposed by Evans. This difference in reaction rates affects the production terms. Thus, production terms for complete Sangiovanni mechanism and for

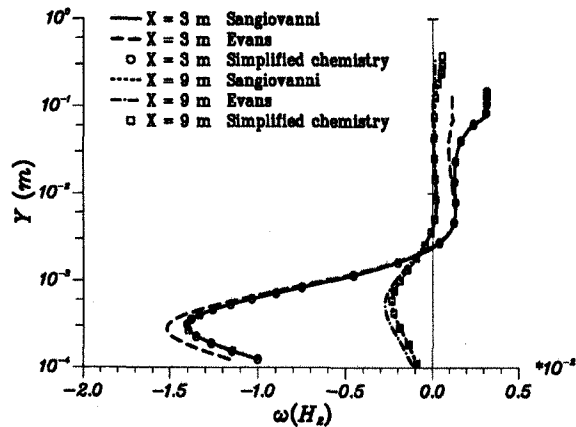


Figure 6: Production terms of species H_2

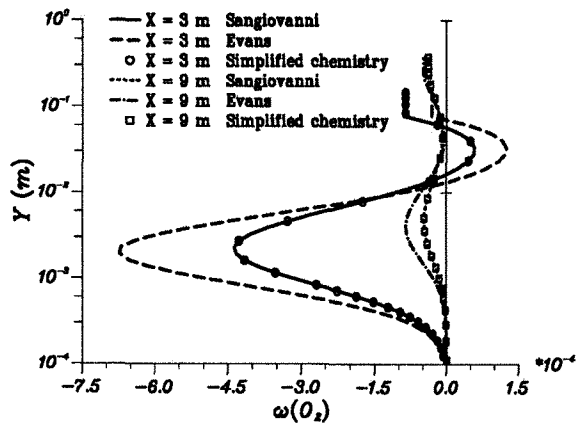


Figure 7: Production terms of species O_2

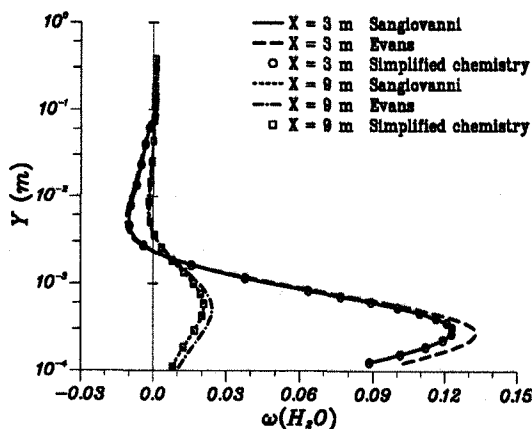


Figure 8: Production terms of species H_2O

the simplified mechanism are identical but differ from the production terms obtained for Evans mechanism. A representation of production terms for a simplified version of Evans model would coincide with production terms for complete Evans mechanism.

It can be seen on figures 6 to 8 that there is destruction of hydrogen and oxygen and production of water near the nozzle wall. When the abscissa X increases, production terms of H_2 , O_2 and H_2O decrease because the combustion of H_2 in air is nearly finished and the temperature of the flow is lower.

Heat flux

Non-equilibrium reactive flows are computed with the complete chemical mechanisms of Sangiovanni and of Evans and with the reduced chemical model given in table 3. In order to evaluate the influence of chemistry, chemically frozen flows are also computed. As no experimental data were available a comparison is made with a turbulent compressible boundary layer code⁽¹⁾. The same turbulence models are implemented, the gas is assumed to be calorically and thermally perfect, the Prandtl number is constant and the viscosity is fitted by a Sutherland type law. In the following figures, this code is referred to as the "ideal gas approach".

The heat flux evolutions, with no turbulence-chemistry interaction, and for the different conditions presented above, are shown in figures 9 to 12.

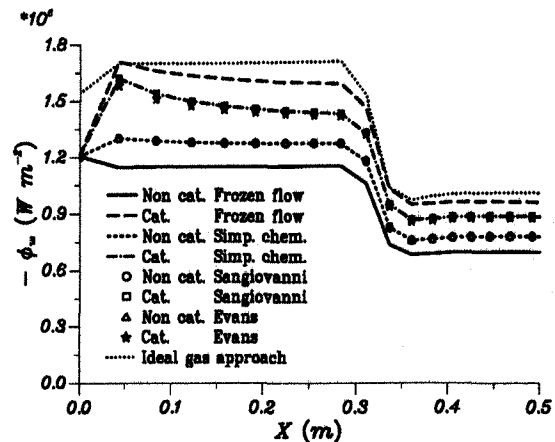


Figure 9: Heat flux at the scramjet exit for $M = 6$, $T_w = 1000K$

There are very high pressure gradients in the beginning of the nozzle expansion. Boundary

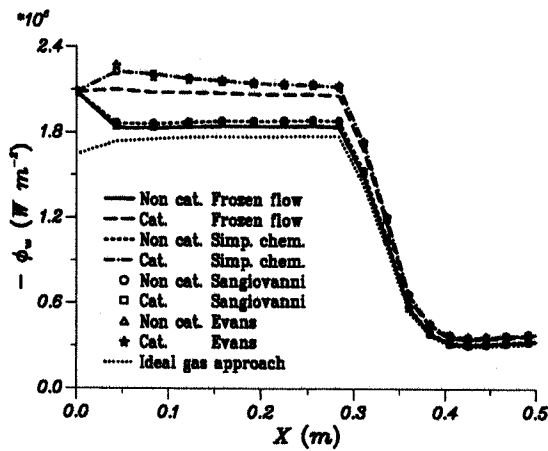


Figure 10: Heat flux at the scramjet exit for $M = 12$, $T_w = 1000K$

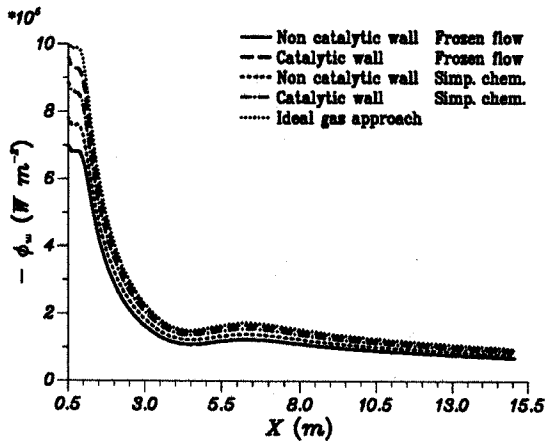


Figure 11: Heat flux along the nozzle for $M = 6$, $T_w = 1000K$

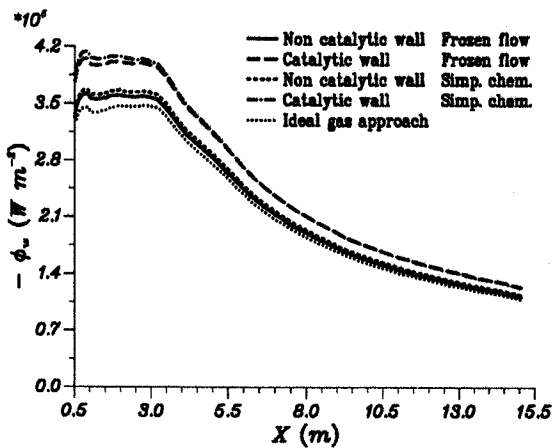


Figure 12: Heat flux along the nozzle for $M = 12$, $T_w = 1000K$

layers are very thin as the flows are highly accelerated, so heat fluxes are much more important in this region, as shown on figures 9 and 10, than in the rest of the nozzle, figures 11 and 12.

Catalycity of the wall have an important effect. Chemical mechanism is globally exothermic and heat flux is higher for a fully catalytic wall than for a non-catalytic one.

As it was previously noticed, reduced chemical mechanism gives the same results as more complete mechanism. The heat fluxes with the two different chemical mechanisms proposed by Sangiovanni and by Evans and with the simplified version of Sangiovanni model cannot be distinguished. Chemistry has less influence on heat flux than the catalycity of the wall in the Mach 12 case and about the same importance in the Mach 6 case.

For a cruise speed of Mach 6, the heat flux distribution presents a maximum of $1.7 \cdot 10^6 \text{ Wm}^{-2}$ at the scramjet exit, then a constant level zone at half value and after, it decreases along the nozzle. For a cruise speed of Mach 12, heat flux at the scramjet exit is higher than in the previous case and the maximum is of $2.2 \cdot 10^6 \text{ Wm}^{-2}$. Heat flux remains very high all along the nozzle. Those high levels of heat flux at the scramjet exit generate a problem of wall cooling at the beginning of the nozzle. Heat flux of respectively $1.7 \cdot 10^6 \text{ Wm}^{-2}$ and $2.2 \cdot 10^6 \text{ Wm}^{-2}$ correspond to black body radiative equilibrium temperatures of about 2340 K and 2500 K, which cannot be supported by the nozzle wall material.

Ideal gas approach is not accurate enough to determine heat fluxes. Errors, on the level of the maximum heat fluxes, of respectively 17 % and 22 % are observed for Mach 6 and Mach 12 cases.

Wall shear stress

Wall shear stress evolutions along the nozzle wall are shown on figures 13 and 14. Wall shear stresses are higher for a cruise speed of Mach 6 than for a cruise speed of Mach 12. For a given Mach number, evolutions are nearly identical for chemically frozen flow, non-equilibrium flow and the ideal gas approach and they are independent of the wall catalycity. So, in order to determine wall shear stress along the nozzle, the ideal gas approach is sufficient.

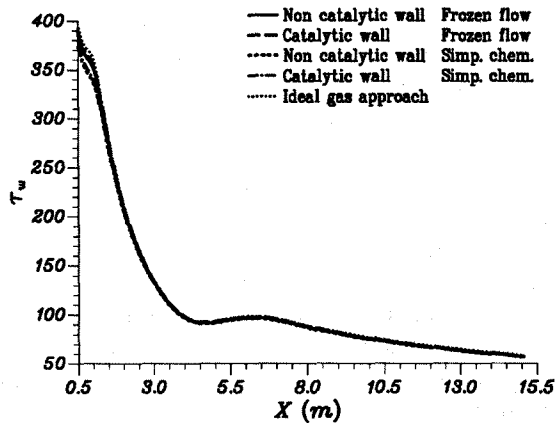


Figure 13: Wall shear stress along the nozzle for $M = 6$, $T_w = 1000K$

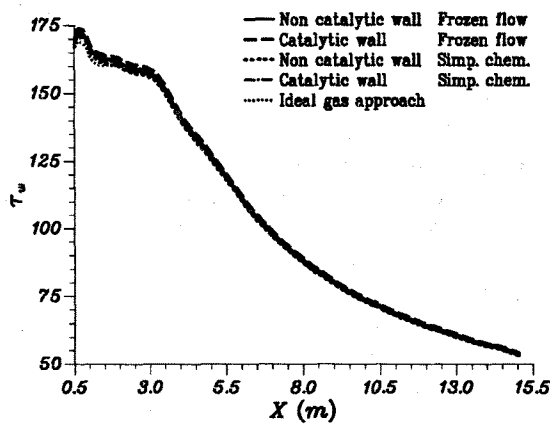


Figure 14: Wall shear stress along the nozzle for $M = 12$, $T_w = 1000K$

Turbulence-chemistry interaction

Noticeable difference between flows with no turbulence-chemistry interaction and flows with temperature fluctuations can only be seen on species mass fractions profiles. Figure 15 shows this effect but, as there are no experimental data, it is not easy to interpret these results.

Heat flux evolutions with turbulence-chemistry interactions are shown on figures 16 and 17. As second order series expansion and assumed Gaussian PDF approaches give identical results, they are represented by the same curves.

Fluctuation intensities, $I = \sqrt{t't'}/\bar{T}$, are under 10 % in the Mach 12 case and even lower in the Mach 6 case. Their influence on the reaction rates is then very weak and heat flux evolutions with temperature fluctuations and

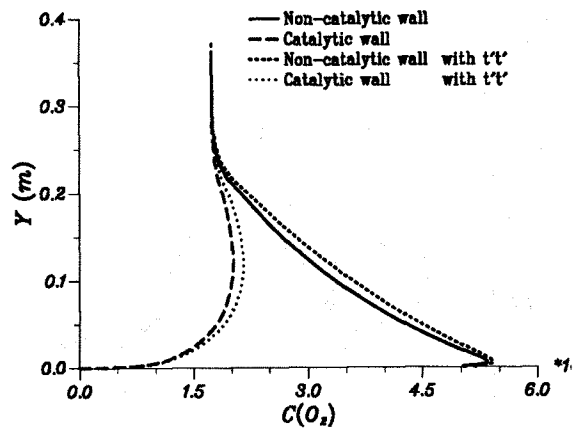


Figure 15: O_2 profiles at $x = 9m$

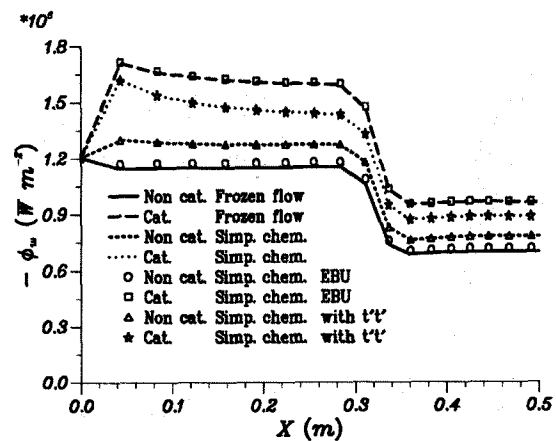


Figure 16: Heat flux at the scramjet exit for $M = 6$, $T_w = 1000K$

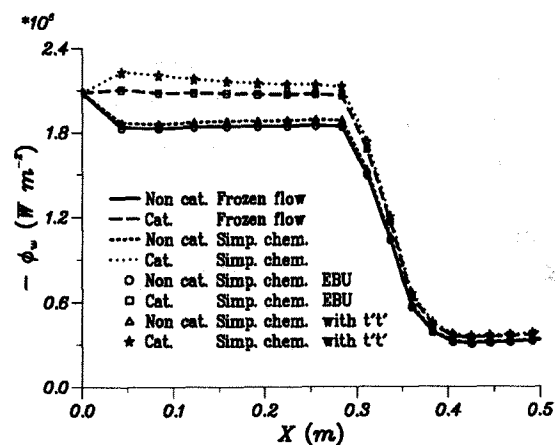


Figure 17: Heat flux at the scramjet exit for $M = 12$, $T_w = 1000K$

with no turbulence-chemistry interaction are very close.

Influence of EBU on heat flux evolutions is very important and curves are merged with the frozen flow curves. In the studied test cases, ω_{ebu} is much more lower than $\omega_{I,r}$ and Eddy-Break-Up model greatly reduces the chemical kinetic. So flows are very close to frozen flows and can hardly be distinguished from them.

Conclusion

A close study of the chemical reaction set succeeds into strongly reduced number of necessary reactions and consequently computation times, with good agreement with complete mechanism results. As the flow at the scramjet exit is not well known, two methods of chemistry-turbulence coupling have to be examined. If the flow is well mixed, chemical reaction rates depend on temperature fluctuations. This can be expressed by using a second order series expansion in $\sqrt{t'/T}$ or a Gaussian type PDF. Both expressions give identical results. At the opposite, if the flow is unmixed, kinetic production rates are limited by turbulent mixing time and chemical production rate are represented by an Eddy-Break-Up model. This leads to a flow very close to frozen flow.

References

- [1] B. Aupoix and D. Arnal. CLIC : calcul des Couches Limites Compressibles, 1988.
- [2] R. Borghi. Chemical reaction calculations in turbulent flows. application to a co-containing turbojet plume. 2nd Symposium IUTAM-IUGG on Turbulent Diffusion in Environmental Pollution, 1973.
- [3] K. Y. Chien. Predictions of channel and boundary-layer flows with a low-Reynolds-number turbulence model. *AIAA Journal*, 20(1), 1982.
- [4] C. Eldem. *Couches limites hypersoniques avec effets de dissociation*. PhD thesis, ENSAE, Toulouse, 1987.
- [5] J. S. Evans and C. J. Schexnayder. Influence of chemical kinetics and unmixedness on burning in supersonic hydrogen flames. *AIAA Journal*, 18(2), 1979.
- [6] W. C. Gardiner, Jr. *Combustion Chemistry*. Springer-Verlag, 1984.
- [7] J. Gaviglio. Reynolds analogies and experimental study of heat transfer in the supersonic boundary layer, 1987.
- [8] U. R. Hattikudur and G. Thodos. Equations for the collision integrals $\Omega^{(1,1)*}$ and $\Omega^{(2,2)*}$. *The Journal of Chemical Physics*, 52, 1970.
- [9] J. O. Hirschfelder, C. F. Curtiss, and R. B. Bird. *Molecular Theory of Gases and Liquids*. John Wiley and Sons, 1954.
- [10] R. J. Kee, F. M. Rupley, and J. A. Miller. The CHEMKIN thermodynamic data base. Sandia report Sand87-8215, Sandia National Laboratories, 1987.
- [11] E. A. Mason and C. S. Saxena. Approximate formula for the thermal conductivity of gas mixtures. *The Physics of Fluids*, 1:361, 1958.
- [12] Y. Nagano and M. Tagawa. An improved $k - \epsilon$ model for boundary layer flows. *Journal of Fluids Engineering - Transactions of the ASME*, 112:33-39, 1990.
- [13] J. R. Narayan and S. S. Girimaji. Turbulent reacting flow computations including turbulence - chemistry interactions. AIAA Paper 92-0342.
- [14] J. J. Sangiovanni, T. J. Barber, and S. A. Syed. The role of hydrogen/air chemistry in nozzle performance simulation for hypersonic propulsion systems. AIAA Paper 90-2492.
- [15] F. Scheid. *Theory and Problems of Numerical Analysis*. Mc Graw-Hill Book Company, 1968.
- [16] D. B. Spalding. Development of the Eddy-Break-Up model of turbulent combustion. 16th Symposium (International) on Combustion, 1976.
- [17] C. R. Wilke. A viscosity equation for gas mixtures. *The Journal of Chemical Physics*, 18(4):517-519, April 1950.
- [18] M. Youssef, Y. Nagano, and M. Tagawa. A two-equation heat transfer model for predicting turbulent thermal fields under arbitrary wall thermal conditions, 1992.